Saudi Journal of Biological Sciences 28 (2021) 2566–2574

Contents lists available at ScienceDirect

Saudi Journal of Biological Sciences

journal homepage: www.sciencedirect.com

Original article

Magnetic field potential effects on the doxorubicin therapeutic activity in Ehrlich tumor growth

Magdy M. Ghannam [a], Hanin A. Al-Otaibi [b], Eman S. Alanazy [c], Doaa Elnagar [d,e], Alaa R. fouad [e], Mohammes S. AlAyed [b], Amany A. Aly [a]

[a] Biophysics Department, Faculty of Science, Cairo University, Egypt
[b] Department of Physics, College of Science, King Saud University, Saudi Arabia
[c] Department of Physics, College of Science, Hail University, Saudi Arabia
[d] Zoology Department, Faculty of Women for Sciences, Arts and Education, Ain Shams University, Cairo, Egypt
[e] Department of Zoology, College of Science, King Saud University, Saudi Arabia

ARTICLE INFO

Article history:
Received 14 August 2020
Revised 24 January 2021
Accepted 27 January 2021
Available online 11 February 2021

Keywords:
Magnetic field
Doxorubicin
Ehrlich tumor
Immunohistochemistry

ABSTRACT

Aim: Therapeutic choices for cancer patients include many combinations of therapeutic protocols. The present study aimed to investigate and discuss the combined effects of magnetic field and chemotherapy treatment on Ehrlich tumor-induced growth in Swiss albino mice. The benefits of both treatments are discussed and interpreted.

Methods: Fifty adult male mice were randomly divided into two groups; ten mice in the first group served as control group and forty in the second group which received a single dose IP injection of tumor fluid (0.02 Ml) to induce tumor. Ten days post injection to allow the tumor to growth, the 40 mice were sub- divided in to 4 sub-groups 10 mice pre each to introduce the treatment.

Results: The results indicated tumor growth inhibition regarding mean tumor volume variation (ml) presented. All treatments display tumor growth prevention effect compared to control untreated mice. Treatment with Dox + 7G (MF) exposure exhibited a significant inhibition of tumor growth than that treated alone with DOX or magnetic field; 82% inhibition for DOX + MF 7 G against 60% for 7 G , and 31% for DOX only. Optical density data show a higher values of the molar absorption coefficient ε for all treated groups than untreated one. The fluorescence emission spectra of Hb show an emission peaks λem at 465, 515, and 639 nm. Hematological examination might indicate to discriminative effects to RBCs, WBCs or/ and Hb for all treated groups. Moreover, treatment with Dox + 7G MF shows a proper discriminative effects than that treatment with DOX or magnetic field only. Osmotic fragility (OF) test indicates that the combination between drug and magnetic field have nontoxic effect against RBCs membrane.

Conclusion: Our findings support further exploration of the potential of magnetic fields in cancer therapeutics, either as adjunct or primary therapy. It may be due to enhancing the drug interaction with tumor cells which increase the therapeutic index of DOX and resulted in increased anti-tumor activity against Ehrlich tumor models. These benefits promote the use of the magnetic field in cancer with chemotherapy over the other traditional treatment agents this highly adapted manner can be used in improving the clinical treatment protocol and fights against cancer.

1. Introduction

Cancer is a significant cause of death throughout the world, though great strides have been made in treatment over the past 50 years. Cancer can be effectively treated by chemotherapy (a complex combination of medications), immunotherapy, radiotherapy, and magnetic field therapy, or a combination of all such

Peer review under responsibility of King Saud University.

Production and hosting by Elsevier

https://doi.org/10.1016/j.sjbs.2021.01.061
1319-562X/

methods (Alshammari et al., 2017; Simon et al., 2008; Ahluwalia and Ahluwalia, 2005; Yeh et al., 2004; Schultz et al., 2003).

Magnetic field therapy aims to suppress tumor growth and has the potential to be a safe alternative to surgical or chemical treatments (Cameron et al., 2014). Lagroye et al. (2011) found a significant decrease in the incidence of leukemia in male rats, but not female, that were exposed intermittently to 1000 mT/60 Hz magnetic fields. They also found that the incidence of malignant lymphoma in female mice that were intermittently exposed to 1000 mT magnetic fields decreased and the incidence of lung tumors in mice of both sexes that were continuously exposed to 200 mT magnetic fields was reduced.

Magnetic fields have been shown to be clinically valuable in a range of the Gauss amplitude for angiogenesis , and exposure to 50-Hz electromagnetic fields (EMFs) alone can prompt apoptosis in cancer cells (Mousavi et al., 2014).

Moreover, magnetic field therapy deprives cancer cells of the necessary oxygen and nutrients, resulting in their death (Cameron et al., 2014).

Using EMF therapy in the early stages of cancer treatment (when cells are proliferating rapidly) may increase the efficacy of anti-cancer agents. The magnetic field produces resistance to cancer cell growth during this stage, although its effectiveness decreases in later stages. This supports the use of magnetic field therapy in the early treatment phase, rather than as a last resort (Lucia et al., 2016). On the other hand, the characteristics of exposure to a magnetic field, such as magnetic frequency, duration, and intensity, play a role in EMFs' biological effects on cancer cells (Q. Han et al., 2018).

Doxorubicin (DOX) is one of several chemotherapy agents used as anti-cancer drugs. DOX is from a class of anthracyclines that was first extracted in the 1970s from Streptomyces peucetius var. A significant limitation of DOX is cytotoxicity, the total cumulative dose being the only criterion currently used to predict toxicity. The cardiotoxicity of the drug is due to its interaction with DNA and the plasma membrane and the participation of many oxidation–reduction reactions. Its harsh side effects, such as cardiomyopathy, can also be lethal. The pathophysiology of DOX cardiomyopathy is predominantly determined by oxidative stress resulting from a disproportion between oxidants and antioxidants (Varshney and Dodke, 2004; Changenet-Barret et al., 2013). There is hope for the development of anthracycline drugs with equal anti-cancer efficacy but less cardiotoxicity (Barenholz, 2012; Thorn et al., 2011).

DOX is intrinsically fluorescent, which makes it suitable for visualization and probing with different technologies of microscopic imaging (Dai et al., 2008).

A static magnetic field (SMF) can prevent cancer cell proliferation, and this effect, combined with anti-neoplastic drugs, is higher than that of anti-cancer drugs or the SMF alone. This combination of chemotherapeutic drugs and SMFs thus has synergistic effects (Gray et al., 2000; Soumaya et al., 2013).

Chen et al. (2010) suggest that SMFs enhance the anti-cancer effects of cisplatin on human leukemic cells, especially when combined with chemotherapy.

The presented work aimed to find and touch the benefits effects of magnetic field on tumor treatment. So the combination effects of magnetic field and chemotherapy treatment on Ehrlich tumor were investigated, discussed and interpreted.

2. Materials

The study was divided into two main parts: drug characterization and in vivo studies.

2.1. Drugs

Doxorubicin hydrochloride (Adriblastina) at a concentration of 2 mg/ml was purchased from Pharmacia Italia S.P.A. (Italy).

2.2. Animals

Fifty normal, healthy male Swiss albino mice were obtained from the Laboratory Animal Centre (College of Pharmacy, King Saud University). They were aged approximately 12 weeks and weighed 20–25 g. A conventional rodent diet and water were provided. The animals were housed at 25 +/− 2 °C.

3. Methods

3.1. Experimental design

2.3.1 Fifty adult mice were randomly divided into two groups; ten mice in the first group served as a healthy control group and forty mice in the second group which received a single dose intraperitoneal of suspension Ehrlich ascites carcinomas cells obtained from the National Cancer Institute "NCI"- Cairo University-Egypt to induce tumor. After transplantation, tumor growth was observed within 4–10 days. Ten days post injection, the second group which have tumor (40 mice) were sub- divided in to 4 sub-groups 10 mice per each as following: Untreated mice, treated with 4 mg/kg doxorubicin three times a week, treated with daily exposure to 7G magnetic field for 5 h and treated with 4 mg/kg doxorubicin three times a week and daily exposure to 7G magnetic field for 5 h. All experimental mice's were dissected 2 weeks post-treatment.

3.2. Tumor induction

The mice were injected intraperitoneal with suspension Ehrlich ascites carcinoma cells (EAC) obtained from the National Cancer Institute (NCI, Cairo University, Egypt). Tumor was maintained by serial transplantation of IP cells. After transplantation, tumor growth was observed for 4–10 days.

3.3. Tumor volume measurement

For evaluating the inhibition of tumor growth, mice of the experimental groups were sacrificed under anesthesia and the ascites fluid from each group was separately gathered in graduated tubes, then the volume was measured (Elbialy et al., 2010).

3.4. Blood preparation

1- For collecting blood, the mice were anesthetized and subjected to cardiac puncture. Blood were collected into sterile tubes with anticoagulant (EDTA) for hematological tests (complete blood count, CBC).

2- Osmotic Fragility (OF) test was conducted by incubation of RBCs in different concentrations of sodium chloride (NaCl, 0–0.9%), at RT for 1 h.

3- To study the blood fluorescence emissions, the absorption spectrum of the mice's blood was directly collected from all the heparinized tubes and prepared as follows. By centrifugation at 2500 rpm at 4 °C for 10 min, erythrocytes (red blood cells) were isolated from the whole blood. Three layers were obtained: RBCs, the buffy coat (BC) layer (the second layer), and platelet-poor plasma (PPP). The BC layer was extracted and stored in another tube with acetone (100 μL (0.1 ml) BC in 5 ml acetone). The RBCs

and PPP were re-centrifuged for 10 min at 3000 rpm at 4 °C to extract the chromophore to be used in the fluorimetric measurements. Packed RBCs were washed with 2 ml of standard saline solution and agitated gently for 2 min, after which they were re-centrifuged to separate the washed RBCs. This step was repeated three times.

3.5. Physical analysis

A. The absorption spectrum

The absorption spectrum of the samples was measured using a UV/Visible Double Beam Spectrophotometer Type 1650 PC (Agilent, Santa Clara, CA, USA) at a wavelength of 200–800 nm.

B. Fluorescence emissions

The fluorescence emission spectra of the samples with different concentrations were measured using a UV/Visible Spectrometer Biochrome-Libra S60PC (Shimadzu, Kyoto, Japan). Several excitation wavelengths (λex) were measured at room temperature.

In this study, fluorescence properties were investigated for all groups. Acetone-suspended blood samples were collected. Blood samples for all groups were excited at 415 nm. Fluorescence emission spectra measurements were taken between 430 and 830 nm, and the emission scanning spectra were recorded (Vishvanath and Ramanujam, 2011; You et al., 2010).

3.6. Biological analysis

3.6.1. Determination of erythrocyte osmotic fragility

The osmotic fragility test (OF) is used to measure erythrocyte resistance to hemolysis while being exposed to varying levels of dilution of a saline solution (Gallagher, 2018; Luba et al., 1989). In the osmotic fragility test, the whole blood is washed many times to remove the hemolyzed cells. So, a certain volume added to a different concentrations of buffered sodium chloride solution and the mixture incubated at room temperature for 1 h.

The mixture was centrifuged and the optical density of the supernatants is measured.

The average percent hemolysis (%) of hemolysis blood cells is calculated using the following formula:

$$\text{Average hemolysis } \% = \frac{\text{average absorption of given conc. of Nacl supernatant}}{\text{average absorption of the 100\% hemolysis supernatant}} \times 100$$

The calculation of Percent hemolysis done based on 100% hemolysis in zero NaCl (100% H_2O) at 540 nm.

3.7. Complete blood count (CBC) test

Blood was collected from each group on the fifth day post-treatment. Measurements were taken for all groups using a hematology analyzer (Beckman Coulter, Nyon, Switzerland) 0.2.5 Histopathological studies

3.8. Histopathological studies

For the histopathological analysis, livers were cut into small pieces and fixed in freshly prepared 10% neutral buffered formalin, dehydrated in ascending grades of ethanol, cleared in xylene, and finally embedded in paraffin wax sections, which were then cut and stained with hematoxylin and eosin.

The liver sections were examined and photographed by light microscopy (Motic 2000, Motic, Xiamen, China). The tumor area and radius were measured by microscopy software and the volume was calculated according to the formula

$$V = \frac{4}{3}\pi r^3$$

3.9. Immunohistochemical localization of Ki 67

Liver sections were deparaffinized in xylene. After that, they were rehydrated in descending series of ethanol and finally distilled water. Then, sections were heated in citrate buffer (PH 6) for 5 min in a microwave and washed with PBS buffer for 5 min three times. Sections were incubated with peroxidase blocking solution for 10 min, followed by primary antibody incubation (anti-Ki 67) overnight at 4 °C.

After washing by PBS, sections were incubated with secondary antibody for 30 min, then incubated with avidin-brotin complex for 30 min, followed by DAB incubation for 10 min. Mayer's hematoxylin was used as the counterstain.

4. Results

4.1. Drug characterization

The drug (doxorubicin, DOX) was prepared at different concentrations of 0.0018, 0.004, 0.006, 0.01, and 0.0138 mg/ml. Fig. 1 shows the absorption spectra of the prepared samples in the wavelength range of 200–800 nm for the different drug concentration. Absorbance spectra of free DOX show an absorption band of around 480 nm, similar to previous studies (You et al., 2010; Dai et al., 2008). The molar absorption coefficient remained constant at 0.24cm^{-1} for DOX. The results indicate that the absorption increases as the drug concentration increases.

Fluorescence emission spectra measurements for all prepared samples were recorded in the wavelength range from 480 up to 500 nm at an excitation of 480 nm for the different drug concentration as shown in Fig. 2. The emitted fluorescence peaked near 595 nm, in agreement with Dai et al. (2008). It is clear from the figures that the fluorescence intensity increased as concentration doses increased.

4.2. In vivo studies

4.2.1. Effect of DOX and magnetic field exposure on tumor volume

The efficacy of drugs (DOX) along with magnetic field treatment used in this study was assessed in vivo, where the tumor fluid was collected and its volume was measured. Fig. 3 shows the volume of the tumor fluid (ml) for untreated and treated groups. It may noted that peritoneal fluid volume was reduced after treatment, especially after magnetic field exposure (DOX + MF 7G, MF 7G), more than conventional treatment by injection only (see Table 1).

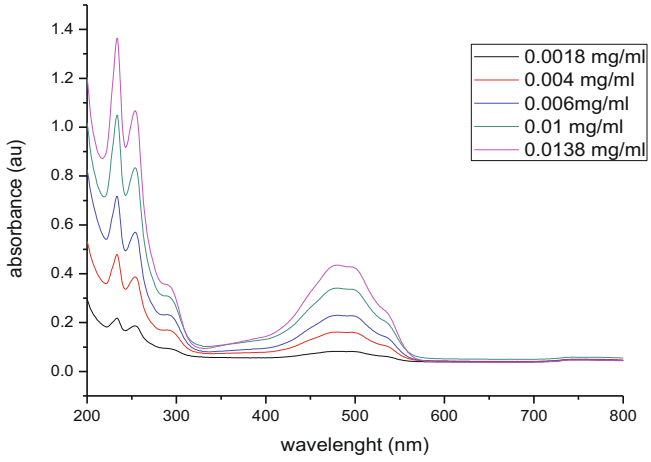

Fig. 1. Absorption spectrum of the drug at different Dox concentrations.

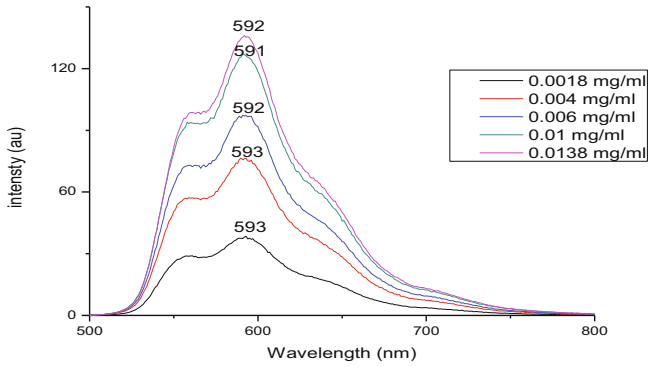

Fig. 2. Fluorescence emission spectrum at different Dox concentrations at 480 nm excitation wavelength.

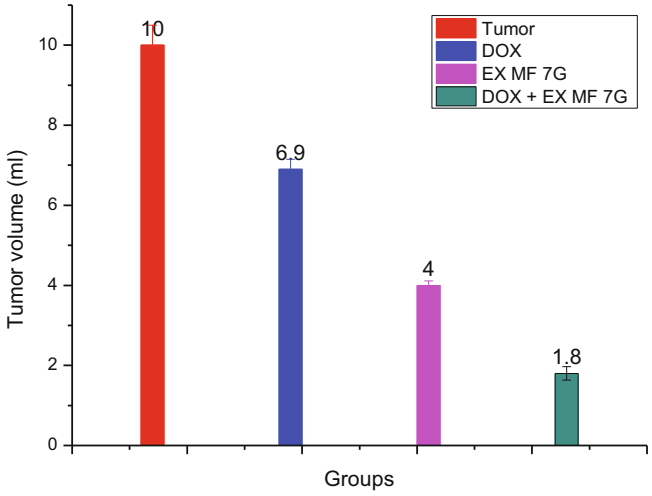

Fig. 3. Average tumor fluid volume for untreated and treated groups.

4.2.2. Effect of DOX and magnetic field exposure on the Hb absorption spectrum.

The absorption spectra were measured in the range of 200–800 nm for all studied groups for all prepared different concentrations. Fig. 4 shows the absorption spectrum for all studied groups at a constant concentration (for example at a concentration of 8%). The hemoglobin absorption spectrum has five characteristic absorbance bands: the Globin band at 274 nm, the Globin band at 344 nm, the Soret band at 415 nm, the Hemo band at 541 nm, and the Hemo band at 576 nm. The Globin band at 344 nm is responsible for Globin–heme interaction, while the Hemo band at 576 nm is responsible for heme–heme interaction. The ratios for all hemoglobin absorbance bands are presented in Table 2. The results demonstrate that absorbance at the bands characteristic

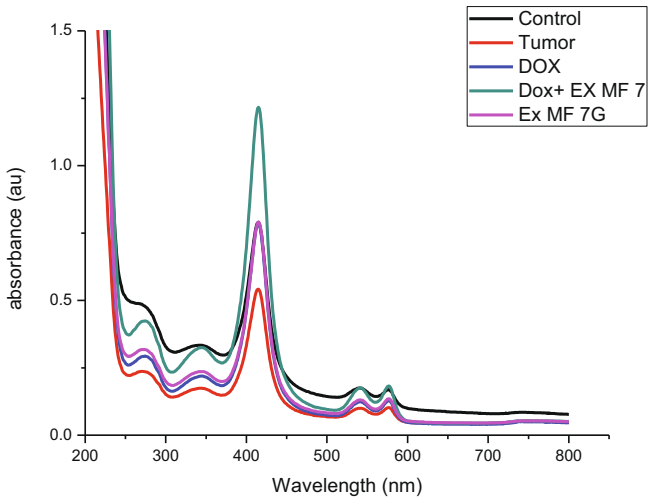

Fig. 4. Hemoglobin absorption spectrum for all studied groups.

increased, and the absorbance ratios of A (576 nm)/A (541 nm), A (415 nm)/A (274 nm), and A (415 nm)/A (576 nm) in the tumor group had larger values than those of the healthy mice. The ratios in the treated groups had larger values than the tumor groups.

Consequently, the hemoglobin molar absorption coefficients were calculated (Table 3). The results show that the molar absorption coefficients are different for all of the studied samples. The molar absorption coefficient for the tumor group is smaller in value than that of the healthy (control) group. The molar absorption coefficients for all the samples from the treated groups are higher than those of the tumor group, which may indicate the effectiveness of the combination of magnetic field and drug therapy in the treatment of tumors.

4.2.3. Effect of treatments on hemoglobin fluorescence emission

In the UV/visible absorption spectrum, porphyrin demonstrates more absorption at around 415 nm (Soret band), while at higher wavelengths (450–700 nm), there is less absorption (Q bands). Considering this fact, the blood samples of all the specimens were excited at 415 nm. Fig. 5 shows the emission spectra of all studied groups. Three peaks are prominent; at 476, 588, and 632 nm (data are summarized in Table 4). The intensity of the peak around 630 nm was more distinct for the control group and the DOX group than that other groups, which in agreement with the changes recorded at this peak (see Fig. 5 and Table 4). Lower fluorescence intensities were observed for the untreated tumor group than for the control group.

Table 4 shows that the emission intensities of the groups treated with 50 μL of Dox only and that treated with 50 μL Dox along with exposing to magnetic field strengths of 7G have value greater

Table 1
Average volume of tumor fluid for treatment groups and untreated group.

Grope name	Start treat, Post injection (Days)	Duration of treatment (Days)	Cancer cell Vol.)Average) (ml)	Note
Tumor) untreated(	Non	Non	10 ± 0.50	Non
DOX Alone	10	7	6.9 ± 0.25	Change color of cancer cell fluid
Exp. 7G MF alone	10	7	4.0 ± 0.11	One mouse has no tumor fluid inside After treatment
DOX + Exp. 7G MF	10	7	1.8 ± 0.17	2 mice do not have tumor fluids inside after treatment

*Values are means ± SEM calculated from n = 3 in each group.

Table 2
The Absorbance bands ratios.

Studied groups	I(576 nm)/I(541)	I(415 nm)/I(576)	I(415 nm)/I(274)
Control	0.965 ± 0.02	4.67 ± 0.63	1.618 ± 0.04
Tumor	1.020 ± 0.10	5.313 ± 0.03	2.29 ± 0.01
Exp. MF 7G	1.048 ± 0.05	7.328 ± 0. 23	3.042 ± 0.20
DOX	1.030 ± 0.01	6.306 ± 0.50	2.734 ± 0.74
DOX + Exp. MF 7G	1.034 ± 0.02	6.686 ± 0.10	2.870 ± 0.46

*Values are means ± SEM calculated from n = 3 in each group.

Table 3
Molar absorption coefficients.

Group	$\varepsilon = \frac{A}{cL}\left(\frac{l}{mole.cm}\right)$
Control	0.019192 ± 0.01
Tumor	0.013114 ± 0.05
Exp. MF 7G	0.032743 ± 0.12
Dox	0.019261 ± 0.05
Dox + Exp. MF 7G	0.020730 ± 0.03

*Values are means ± SEM calculated from n = 3 in each group.

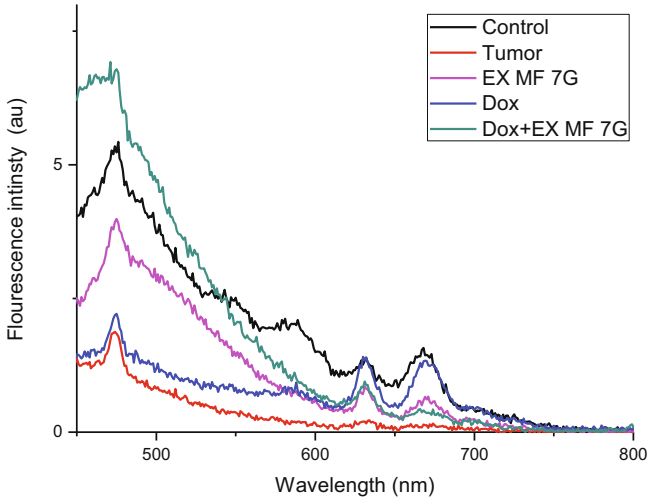

Fig. 5. Blood fluorescence emission spectra for all studied.

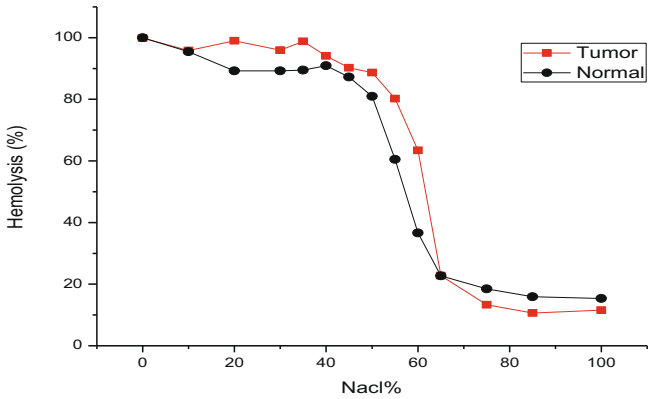

Fig. 6. Osmotic fragility (O.F) curves for healthy (control) and untreated (tumor) groups.

than those for the other groups; which may be due to doxorubicin being natural.

4.2.4. Effect of treatments on erythrocyte osmotic fragility

Fig. 6 shows the osmotic fragility measurement for RBCs collected from mice of control and that of untreated tumor groups. The percentage of hemolysis cells were increasing in untreated group compared to control. The results of the test revealed that the RBC membrane of the group after tumor induction without treatment appeared to lyse in a more fragile manner (was destroyed too quickly) than those of groups exposed to the magnetic field only and the controls. Moreover, the results showed that both the permeability and elasticity of the RBC membrane declined in the treated groups: a group treated only with DOX and the group treated by DOX in combination with magnetic field exposure compared to the group posted tumor induction. By contrast, the group treated with DOX only showed a decrease in osmolality but less than the untreated group, but no effect on RBC fragility was detected compared with the control group. The start and completion of RBC membrane hemolysis for all studied groups are summarized in Table 5.

4.2.5. Effect of treatments on CBC

The blood samples of the group after tumor induction without treatment showed a significantly raised number of WBCs compared to the controls. The group treated with DOX only showed a significant decrease. WBCs increased owing to the tumor. The group exposed to the magnetic field only displayed a decrease in the number of WBCs. Furthermore, the treatment with DOX in combination with magnetic field exposure resulted in a more significant decrease of WBCs. The untreated mice showed a low number of RBCs compared to the controls. By contrast, the group treated with DOX only had an increase of RBCs that decreased owing to the tumor. The group treated by magnetic field only experienced a more significant increase in RBCs. The tumor group that had been subjected to magneto-therapy and DOX treatment displayed an increase in RBCs. Table 6 demonstrates that the mice group post-tumor induction showed a clearly decreased level of Hb compared to the controls. However, both groups treated with DOX only and exposure to magnetic field only exhibited a significant increase in Hgb. In the group treated with combined magnetic field and DOX, increasing HGB levels were found also. According to the results recorded in Table 6, levels of hematocrit for the group after tumor induction decreased compared with the normal group, whereas the group treated with DOX only experienced a significant increase in hematocrit, as did the group treated by magnetic field only. Furthermore, the treatment with DOX in combination with magnetic field exposure resulted in a more significant decrease in hematocrit. The results for platelets (see Table 6) showed a highly raised number in the group post-tumor induction compared to the controls, whereas the group treated with DOX only exhibited a significant decrease in platelets. The mean number of platelets among the mice exposed to the magnetic field only was significantly lower. The treatment with DOX in combination with magnetic field exposure resulted in a significant decrease in thrombocytes.

4.2.6. Effect of DOX and magnetic field on the histopathology of Ehrlich metastasis on the liver

The liver section in the controls showed a normal hepatic structure consisting of a central vein surrounded by strands of hepatocytes separated from one another by sinusoids (Fig. 7A). After tumor induction, Ehrlich metastasis lesions were revealed in the liver tissue. The metastasis was characterized by darkly stained polygonal cells with different degrees of cellular and nuclear pleomorphism besides aggregations of inflammatory cells (Fig. 7B),

Table 4
Peak position and intensities of fluorescence emission spectra of blood for all studied groups.

Groups	λ (nm)	Ints.	λ (nm)	Ints.	λ (nm)	Ints.	I632/I588
Control	476.4	5.36	589.3	2.1	632.5	1.37	0.67
Tumor	473.9	1.9	589.6	0.2	633.1	0.21	1.05
Exp. MF 7G	474.9	3.9	587.2	0.7	631.3	0.83	1.10
DOX	475.0	2.2	588.0	0.9	632	1.39	1.50
DOX + Exp. MF 7G	471.0	6.9	586.9	1.1	633	0.53	0.48

Table 5
Start and completion of RBC membrane hemolysis for all studied groups.

Group	Fragility start	Fragility complete	Start to complete width
Control	65%	40%	25% ± 2%
Tumor	75%	45%	30% ± 1.5%
Exp. MF 7G	75%	50%	25% ± 2%
DOX	65%	45%	20% ± 1.2%
DOX + Exp. MF 7G	60%	45%	15% ± 1.9%

*Values are means ± SEM calculated from n = 3 in each group.

occupying a large area and volume (Table 7). Mice livers treated with DOX after tumor induction showed an improvement, manifested by limited diminished metastatic lesions and neoplastic cells mixed with infiltrative cells compared to the untreated tumor group (Table 7), in addition to dilated and congested veins (Fig. 7C). Moreover, the livers of mice exposed to magnetic field 7G also showed a marked improvement, characterized by the regression of metastatic development, with a few tumor cells captured by inflammatory cells (Fig. 7D), occupying a minimized metastasis area and volume (Table 7). Furthermore, mice livers treated with DOX and exposed to the magnetic field displayed a high regression of metastatic development, represented by partial and completely degenerated metastatic neoplastic cells in the liver tissue around the dilated and congested vein, beside relatively healthy hepatocytes (Fig. 7E), the metastasis areas and volumes being the least among the groups (Table 7).

4.2.7. Immuno-histochemical analysis

The control liver sections showed a negative immune response to Ki-67 antibodies (Fig. 8A) with 0 optical density (Table 8). By contrast, the livers of mice after tumor induction showed a strong immune response, manifested by brown spots (Fig. 8B) with the highest optical density (Table 8). The livers of the mice treated only with DOX revealed less immune response against Ki-67 (Fig. 8C) compared to the untreated tumor group, represented by a few brown spots with lowered optical density (Table 8). Additionally, mice livers exposed to a magnetic field displayed a weak immune response to Ki-67 (Fig. 8D) but with lower optical density (Table 8). Finally, the livers of mice treated with the combination of therapies showed very weak immune response represented by a few small spots (Fig. 8E) with the lowest optical density (Table 8).

5. Discussion

The fluorescence spectra of the free Dox solutions is agree with that obtained by You et al., (2010). UV/visible absorption spectroscopy display that hemoglobin show intense wavelengths absorption (Denninghoff et al., 2007; Faber et al., 2004). The Soret band is characteristic of hematoporphyrin proteins (Chikezie et al., 2013). The Globin band situated at 274 nm (band 1), where the light absorption is due electrons of the aromatic side chain delocalized. The band for Globin-heme at 344 nm (band 2) belongs to the coordinated-covalent bond in iron, and the proximal histidine displays transition. The absorbance band close to 576 nm is thought to be an electronic transition, including the porphyrin ring of the heme group, while the band close to 540 nm is thought to be made out of vibrational transitions (Sherif and Amal, 2010). The results indicate great differences in the absorption spectra of healthy and diseased blood. The absorption spectra for the cancer-diseased mice group have smaller values than those of the healthy mice group. In addition, the absorption values of the treated groups (MF 7G, DOX and DOX + MF 7G) may indicate the therapeutic effectiveness of the combination of magnetic field and drug. Moreover, the increase of the Hemo band (576 nm) and the Globin band (274 nm) in the treated group was more pronounced than in the tumor group (Alshammari et al., 2017). The decrease in the half-Soret bandwidth, which indicates stretching in the bonds of iron and nitrogen in the porphyrin ring and an imbalance between heme and protein in the Hb molecule. The Soret band is sensitive to changes in the microenvironments around the heme site. Previous studies show that, if the protein is denatured (partially or fully), it will result in changing or diminishing the band (Abdelhalim, 2012; El Din et al., 1994). An increase in I(415)/I (274) reflects the presence of free heme (Sherif and Amal, 2010; Selim and El-Marakby, 2010). The displacement of the porphyrin ring from its pocket, which results from radiation exposure, explains the increase in the hemoglobin-oxygen affinity documented previously in several studies (El-Bediwi et al., 2013; Selim and El-Marakby, 2010). The changes in the absorptions' intensity and wavelength result due to variations of the porphyrin

Table 6
Summary of in vivo hematological parameters for blood samples of all groups.

Types	Control	Tumor	DOX	Exp. MF 7G	DOX + Exp. MF 7G
WBCx 10^3/μℓ	5.6 ± 0.45	40.8 ± 0.50	8.7 ± 0.44	28.5 ± 0.23	6.1 ± 0.30
RBCx 10^6/μℓ	8.44 ± 0.50	5.78 ± 0.25	5.82 ± 0.2	6.52 ± 0.40	6.37 ± 0.15
HGB g/dℓ	16.1 ± 0.30	10.2 ± 0.15	11.1 ± 0.43	11.6 ± 0.25	12.4 ± 0.50
HCT %	52.1 ± 0.43	32.5 ± 0.30	36±0.38	34.5 ± 0.25	39.6±0.45
PLT x 10^3/μℓ	413 ± 36.92	891 ± 30.90	753±35.77	633 ± 36.55	798±32.33

*Values are means ± SEM calculated from n = 3 in each group.

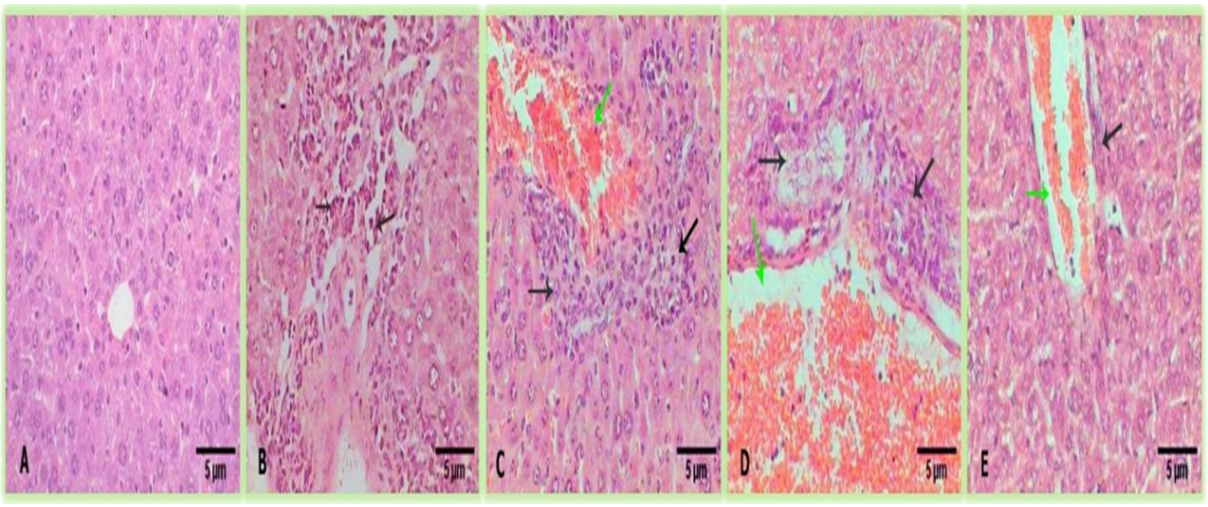

Fig. 7. Photomicrographs of liver sections showing The effect of Dox and magnetic field on hepatic tumor; (A) Control, (B) mice liver after tumor induction revealing great aggregations of tumor cells and leukocyte infiltration (black arrows), (C) mice liver, Post-treated with Dox (4 mg/kg) showing less tumor lesion (black arrows) Congested and dilated portal vein (green arrow), (D) mice liver exposed to magnetic field after tumor induction displaying degenerated tumor lesions (black arrows), congest and dilated portal vein (green arrow), (E) mice liver post- treated with Dox (4 mg/kg) and exposed to magnetic field 7 G revealing very small degenerate tumor lesion (black arrow) Congested and dilated Portal vein (green arrow) (H&E-400X).

Table 7
Areas and volumes of metastasis in untreated group after induction of tumor and in the post-treatment groups.

Groups	Area (µm)	Volume (µm)
Control	0 ± 0	0 ± 0
Tumor	0.60 ± 0.06	0.34 ± 0.05
Dox	0.30 ± 0.04	0.11 ± 0.02
EX MF 7G	0.2 0 ± 0.02	0.04 ± 0.01
Dox + EX MF 7G	0.10 ± 0.01	0.02 ± 0.01

*Values are means ± SEM calculated from n = 3 in each group.

ring's peripheral substituents. The inclusion of metal into the porphyrin cavity or protonation of the two inner nitrogen atoms also results in changes to the visible absorption spectrum; these absorptions are used to determine specific features on a porphyrin (Courrol et al., 2007). The prominent peak at 632 nm indicates a neutral form of porphyrin. In addition, the peak at 476 nm is produced by acetone (due to the C–H vibrations of acetone) and heparin. Raman scattering is seen significantly in lower concentrations of the blood (Han et al., 2016; Kalaivani et al., 2008; Masilamani et al., 2012 & 2004).

Decreasing fluorescence intensities which observed in the untreated tumor group is consistent with Weber et al. (2013). Lower fluorescence intensities were observed for the untreated tumor group than the control which in consistent with previous finding (Weber et al., 2013; Vishvanath and Ramanujam, 2011; Kalaivani et al., 2008(. This may be explained by the huge number of cancer cells in blood control group, which may cause fluorescence quenching. The blood fluorescence emission may change in cancer cases, showing distinct peaks (around 630 nm) due to the porphyrin fluorophore (Kalaivani et al., 2008; Courrol et al., 2007). Porphyrin fluorescence in the neoplastic was lower or higher than in normal depending on their nature. There was probably a decrease in the 588 nm region as cells progress from a normal to a cancerous state (Khan et al., 2015; Vishvanath and Ramanujam, 2011). These values are less for the control group but at their maximum for cancer patients. Normal porphyrin was elevated for the patients, consistent with previous results (see Table 4) (Kalaivani et al., 2014). Weber and co-workers (2013) use the methods of fluorescence spectroscopy to examine and measure the uptake of DOX chemotherapeutic drug in human breast cancer cells. They noticed a higher intensities of fluorescence that indicate increase drug uptake and more drug responses

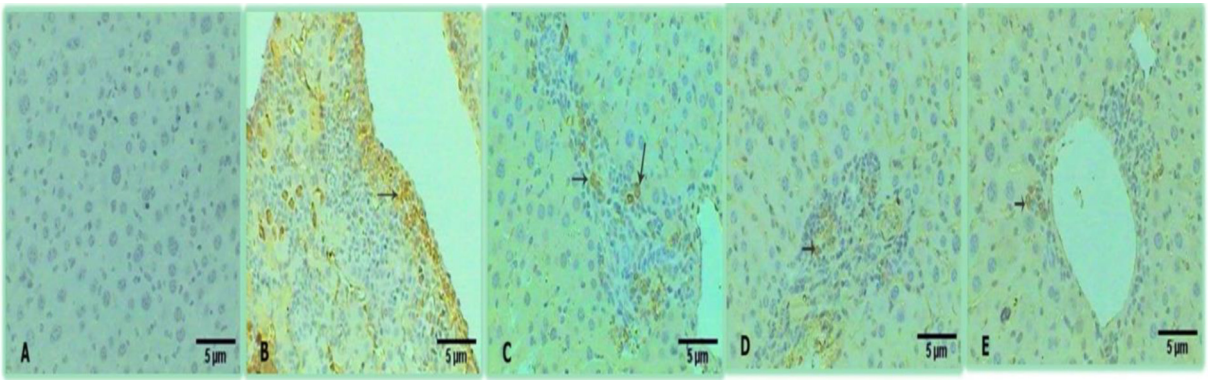

Fig. 8. Photomicrographs of mice liver sections showing the immune response against Ki-67; (A) No immune response in Control liver, (B) strong immune response in the untreated group after tumor induction (arrows), (C) slight immune response in the group post-treated with Dox (4 mg/kg) after tumor induction (D) week immune response in the group exposed to magnetic field 7G (arrow), (E) immune response in the group post treated with Dox (4 mg/kg) and exposed magnetic field 7G. (ABC – 400x).

Table 8
Optical density of the livers of the tumor groups Ki-67 of control, untreated tumor and treated tumor groups.

Groups	Optical Density
Control	0.0 ± 0.0
Tumor	0.9 ± 0.03
Dox	0.5 ± 0.01
EX MF 7G	0.06 ± 0.02
Dox + EX MF 7G	0.04 ± 0.03

*Values are means ± SEM calculated from n=3 in each group.

were concomitant with higher membrane fluidity. The untreated cells showed lower fluorescence intensities than the cells treated by DOX which is consistent with the changes recorded in this study which demonstrate that the intensity values of the group treated with only 50 μL DOX and the group treated with 50 μL DOX and exposure to constant magnetic field strengths of 7G were greater than those for the untreated tumor group.

Coldman and coworkers (1969) considered that the amount of hemoglobin (Hb) released is a quantitative measure number of the of lysed RBCs. The O.F curve reflects a decreased or increased of hemolysis of RBCs depending on left or right shift respectively (Cueff et al., 2010; Coldman et al., 1969) which means the sooner hemolysis occurs, the greater the osmotic fragility of the cells.

In dynamic changes of osmotic fragility curves, the likely assumption is that right or left shifts indicate a increased or decreased state of cells hydration, respectively. This result in direct affect on membrane transport from osmotic fragility measurements (see Fig. 6). (Cueff et al., 2010)

Its known that the erythrocyte surface area normally remains fixed as its volume increases or decreases, this make erythrocyte suitabile for studies of membrane function. In hypotonic solutions, erythrocytes get swell until a point where is additional increase in volume results in rupture of the cell membrane.In normal erythrocytes, this hemolytic is resposible for approximately to a 70% increase in cell volume. (Dumont et al., 1977)

The calculated average (mean) of O.F data for all groups show clearly the difference between groups especially the rapid hemolysis occurs within a range of NaCl percent (75%−50%) for all groups. The NaCl concentration (C%) percentage where hemolysis starts to occur characterized by water molecules transportation through the RBCs membrane and hence its permeability. The decrease of the values of C% indicates the decrease in the membrane permeability. Cancer cells affecting on RBCs fragility (Tumor) group. The RBCs in tumor group were more fragile (destroyed too quickly) than RBCs in (control) healthy group (Kolanjiappan et al., 2002). RBCs from mice with with Ehrlich ascites tumor significantly undergo an alteration in some cell membrane component that regulates either cations permeability and water or the cell distensibility (Dumont et al., 1977). This is due to the free radical mediate oxidative stress causing lipid peroxidation and seen in cancer and other diseases. In normal aerobic conditions, RBCs are exposed to oxidative stress which is neutralized by enzymatic and non-enzymatic antioxidant system. Any disturbance in these may leads to decrease capillary perfusion and result in cell lysis (Nandhakumar et al., 2013; Kolanjiappan et al., 2002).

The results demonstrate the membrane hemolysis is accrued in higher Nacl concentration in cancer patients. On the other hands, this change in RBC's properties may be reflected on some failure of the RBC's metabolic activity.

Moreover, The results demonstrate that : RBCs membrane permeability and elasticity both are increased due to exposure to magnetic field. This indicates that exposure to the magnetic field can cause changes in Hb molecules structurs and hence the physiological functions of RBC's ((Hassan and Abdelkawi, 2010; Ali et al., 2003). Szwarocka and Jóźwiak (1999) demonstrated that Daunorubicin drug as an anthracycline antibiotics did not induce changes in the fluidity (also refers to fragility) of RBCs membranes. Moreover, they did not exclude the possibility of using erythrocytes (RBCs) as carriers of anthracycline antibiotics (Szwarocka and Jóźwiak, 1999).

In summary, the O.F experiment indicates deformability of RBCs membranes as a result of cancer. In this experiment, treatment the cancer with various anticancer treatments (DOX, MF7G) showed decreases in O.F comparable with tumor group, This could be enhanced with CBC results and suggest that these drugs (DOX) and magnetic field sustain therapeutic value of inhibit tumor growth with the cleared nontoxic hematologic profile.

The decrease in (WBCs) counts in treated groups (DOX, MF 7 G, DOX MF7G) might point out to some improvement in the immune system due to treatments indicates the effectiveness of the magnetic field and drugs in the treatment of tumors.

Most of studies on intraperitoneal inoculation with Ehrlich ascites resulted in liver, lung, spleen and kidney metastasis. It is might be attributed to the migration of tumor cells in the ascetic fluid through the peritoneal cavity and induce soft organs metastasis (Aldubayan et al., 2019; Mishra et al., 2018). The present results is consistent with the previous findings, that induction of Ehrlich ascites lead to performance of liver metastasis manifested by aggressive polymorphic neoplastic cells in the liver tissue.

Doxorubicin is an effective anti-biotic and anti-tumor drug. It has been formulated for the treatment of liver and kidney carcinoma besides to breast cancer metastasis (Alkhatib et al., 2018). Accordingly, these findings reported that DOX treatment resulted in inhibition of the hepatic metastasis. These approach indicated that exposure of mice to magnetic field inhibited the progression of Ehrlich metastasis in the liver that coincided with Tatarov et al. (2011) who suggested the potent role of magnetic field in tumor therapy and speculated that suppression of tumor growth may be attributed to suppression of angiogenesis. On the other hand, many studies were performed to enhance the activity of DOX by herbal extracts (Abd Elrazik et al., 2019; Aldubayan et al., 2019). The present work suggested the exposure to magnetic field with DOX treatment to get more efficiency and effectiveness on the hepatic metastasis due to Ehrlich inoculation. The results indicated marked inhibition for hepatic metastasis progression manifested by degenerated neoplastic cells and relatively healthy liver tissue.

It appears that there are many factors that influence the effects of MF on the tumor growth. These include the type, strength of MF and duration of exposure. However, MFs penetrate the body and act on all organs, altering the cell membrane potential and the distribution of ions and dipoles. These alterations may influence biochemical processes in various metabolic ways.

6. Conclusion

Our findings support further exploration of the potential of magnetic fields in cancer therapeutics, either as adjunct or primary therapy. It may be due to enhancing the drug interaction with tumor cells which increase the therapeutic index of DOX and resulted in increased anti-tumor activity against Ehrlich tumor models. These benefits promote the use of the magnetic field in cancer with chemotherapy over the other traditional treatment agents which can be used in improving the clinical treatment protocol and fights against cancer.

6.1. Statistical data analysis

Data analysis was carried out with the software package, Microsoft Excel, Version 2010 and origin software, version 8.1 (Northampton, Massachusetts, USA). Results are expressed as mean ± standard error (n = 10, independent samples).

Declaration of Competing Interest

There are no conflicts of interest.

References

Abd Elrazik, N., El-Mesery, M., El-Karef, A., Eissa, L., El Gayar, A., 2019. Chlorogenic acid potentiates antitumor effect of doxorubicin through upregulation of death receptors in solid Ehrlich carcinoma model in mice. Egypt. J. Basic Appl. Sci. 6 (1), 158–172. https://doi.org/10.1080/2314808x.2019.1682331.

Abdelhalim, M.A.K., 2012. The bioaccumulation and toxicity induced by gold nanoparticles in rats in vivo can be detected by ultraviolet-visible (UV-visible) spectroscopy. Afr. J. Biotechnol. 11 (39), 9399–9406.

Ahluwalia, V.K., Ahluwalia, M., 2005. Cancer Causes and Prevention. Lotus Press.

Aldubayan, M.A., Elgharabawy, R.M., Ahmed, A.S., Tousson, E., 2019. Antineoplastic activity and curative role of avenanthramides against the growth of Ehrlich solid tumors in mice. Oxid. Med. Cell. Longevity 2019. https://doi.org/10.1155/2019/5162687.

Ali, F.M., Mohamed, S.W., Mohamed, M.R., 2003. Effect of 50 Hz, 0.2 mT magnetic fields on RBC properties and heart functions of albino rats. Bioelectromagnet.: J. Bioelectromagnetics Soc., Soc. Phys. Regulat. Biology Med., Eur. Bioelectromagnet. Assoc. 24 (8), 535–545.

Alkhatib, M., Alshehri, W., Abdu, F., 2018. In vivo evaluation of the anticancer activity of the gemcitabine and doxorubicin combined in a nanoemulsion. J. Pharmacy Bioallied Sci. 10, 35. https://doi.org/10.4103/jpbs.JPBS_225_17.

Alshammari, F.M., Reda, S.M., Ghannam, M.M., 2017. Potential effects of gamma irradiation on the stability and therapeutic activity of anticancer drug, doxorubicin. J. Radiat. Res. Appl. Sci. 10 (2), 103–109.

Barenholz, Y.C., 2012. Doxil®—the first FDA-approved nano-drug: lessons learned. J. Control. Release 160 (2), 117–134.

Cameron, I.L., Markov, M.S., Hardman, W.E., 2014. Optimization of a therapeutic electromagnetic field (EMF) to retard breast cancer tumor growth and vascularity. Cancer Cell Int. 14 (1), 125.

Changenet-Barret, P., Gustavsson, T., Markovitsi, D., Manet, I., Monti, S., 2013. Unravelling molecular mechanisms in the fluorescence spectra of doxorubicin in aqueous solution by femtosecond fluorescence spectroscopy. PCCP 15 (8), 2937–2944.

Chen, W.-F., Qi, H., Sun, R.-G., Liu, Y., Zhang, K., Liu, J.-Q., 2010. Static magnetic fields enhanced the potency of cisplatin on K562 cells. Cancer Biother. Radiopharm. 25 (4), 401–408.

Chikezie, P., Akuwudike, A., Chilaka, F., 2013. Absorption spectra of normal adults and patients with sickle cell anaemia haemoglobins treated with hydrogen peroxide at two pH values. Iranian J. Blood Cancer 5 (4), 129–135.

Coldman, M.F., Gent, M., Good, W., 1969. The osmotic fragility of mammalian erythrocytes in hypotonic solutions of sodium chloride. Comp. Biochem. Physiol. 31 (4), 605–609.

Courrol, L.C., de Oliveira Silva, F.R., Coutinho, E.L., Piccoli, M.F., Mansano, R.D., Júnior, N.D.V., Schor, N., Bellini, M.H., 2007. Study of blood porphyrin spectral profile for diagnosis of tumor progression. J. Fluorescence 17 (3), 289–292.

Cueff, A., Seear, R., Dyrda, A., Bouyer, G., Egée, S., Esposito, A., Skepper, J., Tiffert, T., Lew, V.L., Thomas, S.L.Y., 2010. Effects of elevated intracellular calcium on the osmotic fragility of human red blood cells. Cell Calcium 47 (1), 29–36.

Dai, X., Yue, Z., Eccleston, M.E., Swartling, J., Slater, N.K.H., Kaminski, C.F., 2008. Fluorescence intensity and lifetime imaging of free and micellar-encapsulated doxorubicin in living cells. Nanomed. Nanotechnol. Biol. Med. 4 (1), 49–56.

Denninghoff, K.R., Chipman, R.A., Hillman, L.W., 2007. Blood oxyhemoglobin saturation measurements by blue-green spectral shift. J. Biomed. Opt. 12 (3), 34020.

Dumont, A.E., Nachbar, M.S., Martelli, A.B., 1977. Altered erythrocyte osmotic fragility in mice with Ehrlich ascites tumor. J. Natl Cancer Inst. 59 (3), 989–991.

El Din, S., Aisha, A., El Bahay, A.Z., 1994. Effect of gamma irradiation on infrared spectra of rat hemoglobin. Radiat. Phys. Chem. 44 (1–2), 195–197.

El-Bediwi, A.B., Saad, M., El-kott, A.F., Eid, E., 2013. Influence of electromagnetic radiation produced by mobile phone on some biophysical blood properties in rats. Cell Biochem. Biophys. 65 (3), 297–300.

Elbialy, N., Abdelhamid, M., Youssef, T., 2010. Low power argon laser-induced thermal therapy for subcutaneous Ehrlich carcinoma in mice using spherical gold nanoparticles. J. Biomed. Nanotechnol. 6 (6). 687–693.147.

Faber, D.J., Aalders, M.C.G., Mik, E.G., Hooper, B.A., van Gemert, M.J.C., van Leeuwen, T.G., 2004. Oxygen saturation-dependent absorption and scattering of blood. Phys. Rev. Lett. 93 (2), 28102.

Gallagher, P.G., 2018. Red blood cell membrane disorders. In: Hoffman, R., Benz, E.J., Silberstein, L.E. (Eds.), Hematology: Basic Principles and Practice. 7th ed. Elsevier;:chap 45, Philadelphia, PA.

Gray, J.R., Frith, C.H., Parker, J.D., 2000. In vivo enhancement of chemotherapy with static electric or magnetic fields. Bioelectromagnet.: J. Bioelectromagnet. Soc., Soc. Phys. Regul. Biol. Med., Eur. Bioelectromagnet. Assoc. 21 (8), 575–583.

Han, Q., Chen, R., Wang, F., Chen, S., Sun, X., Guan, X., Yang, Y., Peng, B., Pan, X., Li, J., 2018. Pre-exposure to 50 Hz-electromagnetic fields enhanced the antiproliferative efficacy of 5-fluorouracil in breast cancer MCF-7 cells. PLoS ONE 13 (4).

Han, C., Liu, Y., Yao, Y., Wu, Q., Li, D., Yan, C., Qu, L., Lv, S., Li, H., 2016. Blood fluorescence polarization characteristics of saturated fatty acid biological effects. Optik 127 (24), 11877–11883.

Hassan, N.S., Abdelkawi, S.A., 2010. Changes in molecular structure of hemoglobin in exposure to 50 Hz magnetic fields. Nature 8 (8), 236–243.

Kalaivani, R., Masilamani, V., Sivaji, K., Elangovan, M., Selvaraj, V., Balamurugan, S. G., Al-Salhi, M.S., 2008. Fluorescence spectra of blood components for breast cancer diagnosis. Photomed. Laser Surg. 26 (3), 251–256.

Kalaivani, Rudran, Masilamani, V., AlSalhi, M.S., Devanesan, S., Ramamurthy, P., Palled, S.R., Ganesh, K.M., 2014. Cervical cancer detection by time-resolved spectra of blood components. J. Biomed. Opt. 19 (5), 57011.

Khan, H.B.H., Vani, S., Palanivelu, S., Panchanadham, S., 2015. Erythrocyte protoporphyrin fluorescence as a biomarker to monitor the anticancer effect of Semecarpus Anacardium in DMBA induced mammary carcinoma rat model. J. Fluorescence 25 (4), 907–915.

Kolanjiappan, K., Manoharan, S., Kayalvizhi, M., 2002. Measurement of erythrocyte lipids, lipid peroxidation, antioxidants and osmotic fragility in cervical cancer patients. Clin. Chim. Acta 326 (1–2), 143–149.

Lagroye, I., Percherancier, Y., Juutilainen, J., De Gannes, F.P., Veyret, B., 2011. ELF magnetic fields: animal studies, mechanisms of action. Prog. Biophys. Mol. Biol. 107 (3), 369–373.

Luba, Judkiewicz, Bartosz, Grzegorz, Oplatowska, Anna, Oplatowska, Anna, 1989. Modified osmotic fragility test for the laboratory diagnosis of hereditary spherocytosis. Am. J. Hematol. 31 (2), 136–137.

Lucia, U., Ponzetto, A., Deisboeck, T.S., 2016. Constructal approach to cell membranes transport: Amending the 'Norton-Simon'hypothesis for cancer treatment. Sci. Rep. 6, 19451.

Masilamani, Vadivel, AlSalhi, M.S., Vijmasi, T., Govindarajan, K., Rai, R.R., Atif, M., Prasad, S., Aldwayyan, A., 2012. Fluorescence spectra of blood and urine for cervical cancer detection. J. Biomed. Opt. 17 (9), 98001.

Masilamani, V., Al-Zhrani, K., Al-Salhi, M., Al-Diab, A., Al-Ageily, M., 2004. Cancer diagnosis by autofluorescence of blood components. J. Lumin. 109 (3–4), 143–154.

Mishra, S., Tamta, A.K., Sarikhani, M., Desingu, P.A., Kizkekra, S.M., Pandit, A.S., Kumar, S., Khan, D., Raghavan, S.C., Sundaresan, N.R., 2018. Subcutaneous Ehrlich Ascites Carcinoma mice model for studying cancer-induced cardiomyopathy. Sci. Rep. 8 (1), 1–11. https://doi.org/10.1038/s41598-018-23669-9.

Mousavi, M., Baharara, J., Shahrokhabadi, K., 2014. The synergic effects of Crocus sativus L. and low frequency electromagnetic field on VEGFR2 gene expression in human breast cancer cells. Avicenna J. Med. Biotechnol. 6 (2), 123.

Nandhakumar, R., Kasinathan, N.K., Sivasithamparam, N.D., 2013. Protective role of morin on the attenuation of chemotherapeutic agent, 5-fluorouracil, induced biochemical alterations in erythrocyte membrane–an in vivo animal study. Biomed. Prevent. Nutrit. 3 (1), 19–25.

Schultz, P.N., Beck, M.L., Stava, C., Vassilopoulou-Sellin, R., 2003. Health profiles in 5836 long-term cancer survivors. Int. J. Cancer 104 (4), 488–495.

Selim, N.S., El-Marakby, S.M., 2010. Radiation-induced changes in the optical properties of hemoglobin molecule. Spectrochim. Acta Part A Mol. Biomol. Spectrosc. 76 (1), 56–61.

Sherif, S.M., Amal, E.I., 2010. Analysis of retinal b-wave by fourier transformation due to ammonia exposure and the role of blood erythrocytes. Romanian J. Biophys. 20, 269–281.

Simon, C., Watson, M., Drake, A., Fenton, A., McLoughlin, C., 2008. Principles of cancer treatment. InnovAiT.

Soumaya, LaGhodbanehbib, A., Sakly, M., Abdelmelek, H., 2013. Bioeffects of static magnetic fields: oxidative stress, genotoxic effects, and cancer studies. BioMed Res. Int. 2013.

Szwarocka,A.,Jóźwiak,Z.,1999.Theeffectofdaunorubicinandglutaraldehydetreatment on the structure of erythrocyte membrane. Int. J. Pharm. 181 (1), 117–123.

Tatarov, I., Panda, A., Petkov, D., Kolappaswamy, K., Thompson, K., Kavirayani, A., Lipsky, M.M., Elson, E., Davis, C.C., Martin, S.S., Detolla, L.J., 2011. Tatarov etal 2011_Effects of alternate Mag field to breast cancer. 61(4), 339–345.

Thorn, C.F., Oshiro, C., Marsh, S., Hernandez-Boussard, T., McLeod, H., Klein, T.E., Altman, R.B., 2011. Doxorubicin pathways: pharmacodynamics and adverse effects. Pharmacogenet. Genomics 21 (7), 440.

Varshney, L., Dodke, P.B., 2004. Radiation effect studies on anticancer drugs, cyclophosphamide and doxorubicin for radiation sterilization. Radiat. Phys. Chem. 71 (6), 1103–1111.

Vishvanath, K., Ramanujam, N., 2011. Fluorescence Spectroscopy in Vivo. Encyclopedia of Analytical Chemistry. John Wiley & Sons Ltd, Chichester, p. 1.

Weber, P., Wagner, M., Schneckenburger, H., 2013. Cholesterol dependent uptake and interaction of doxorubicin in MCF-7 breast cancer cells. Int. J. Mol. Sci. 14 (4), 8358–8366.

Yeh, E.T.H., Tong, A.T., Lenihan, D.J., Yusuf, S.W., Swafford, J., Champion, C., Durand, J.-B., Gibbs, H., Zafarmand, A.A., Ewer, M.S., 2004. Cardiovascular complications of cancer therapy: diagnosis, pathogenesis, and management. Circulation 109 (25), 3122–3131.

You, J., Zhang, G., Li, C., 2010. Exceptionally high payload of doxorubicin in hollow gold nanospheres for near-infrared light-triggered drug release. ACS Nano 4 (2), 1033–1041.